# The Impact of Photopigment Bleaching on the Human Rod Photoreceptor Subretinal Space Measured Via Optical Coherence Tomography

Alina Messner,[1,2] Valentin Aranha dos Santos,[1] Stefan Puchner,[1] Hannes Stegmann,[1] Andreas Schlatter,[3,4] Doreen Schmidl,[3] Rainer Leitgeb,[1] Leopold Schmetterer,[1,3,5–9] and René M. Werkmeister[1]

[1]Center for Medical Physics and Biomedical Engineering, Medical University of Vienna, Vienna, Austria
[2]Department of Biomedical Imaging and Image-guided Therapy, Medical University of Vienna, Vienna, Austria
[3]Department of Clinical Pharmacology, Medical University of Vienna, Vienna, Austria
[4]Vienna Institute for Research in Ocular Surgery (VIROS), Department of Ophthalmology, Hanusch Hospital, Vienna, Austria
[5]Singapore Eye Research Institute, The Academia, Singapore, Singapore
[6]School of Chemistry, Chemical Engineering and Biotechnology, Nanyang Technological University, Singapore, Singapore
[7]SERI-NTU Advanced Ocular Engineering (STANCE), Singapore, Singapore
[8]Ophthalmology and Visual Sciences Academic Clinical Program, Duke-NUS Medical School, Singapore
[9]Institute of Molecular and Clinical Ophthalmology, Basel, Switzerland

Correspondence: René M. Werkmeister, Medical University of Vienna, Center for Medical Physics and Biomedical Engineering, Währinger Gürtel 18-20/4L, Vienna A-1090, Austria; rene.werkmeister@meduniwien.ac.at.

**Received:** August 30, 2023
**Accepted:** February 27, 2024
**Published:** March 12, 2024

Citation: Messner A, Aranha dos Santos V, Puchner S, et al. The impact of photopigment bleaching on the human rod photoreceptor subretinal space measured via optical coherence tomography. *Invest Ophthalmol Vis Sci.* 2024;65(3):20. https://doi.org/10.1167/iovs.65.3.20

**Purpose.** The purpose of this study was to investigate rod photopigment bleaching-driven intrinsic optical signals (IOS) in the human outer retina and its measurement repeatability based on a commercial optical coherence tomography (OCT) platform.

**Methods.** The optical path length of the rod photoreceptor subretinal space (SRS), that is, the distance between signal bands of rod outer segment tips and retinal pigment epithelium, was measured in 15 healthy subjects in ambient light and during a long-duration bleaching white-light exposure.

**Results.** On 2 identical study days (day 1 and day 2 [D1 and D2]), light stimulation resulted in a significant decrease in rod SRS by 21.3 ± 7.6% and 19.8 ± 8.5% (both $P < 0.001$), respectively. The test-retest reliability of the SRS maximum change of an individual subject was moderate for single measures (intraclass correlation coefficient [ICC] = 0.730, 95% confidence interval [CI] = 0.376, 0.900, $P < 0.001$) and good for average measures (ICC = 0.844, 95% CI = 0.546, 0.947, $P < 0.001$). The mean area under the stimulus response curve with values of 14.8 ± 9.4 and 15.5 ± 7.5 µm × minutes ($P = 0.782$) showed excellent agreement between the stimulus response on D1 and D2. Intermittent dark adaptation of the retina led to an initial increase of the SRS by 6.1% ($P = 0.018$) and thereafter showed a decrease toward baseline, despite continued dark adaptation.

**Conclusions.** The data indicate the potential of commercial OCT in measuring slow IOS in the outer retina suggesting that the rod SRS could serve as a biomarker for photoreceptor function. The presented approach could provide an easily implementable clinical tool for the early detection of diseases affecting photoreceptor health.

Keywords: optophysiology, intrinsic optical signal (IOS), subretinal space (SRS), optical coherence tomography (OCT), photoreceptors

Optical coherence tomography (OCT) is an imaging technique yielding cross-sectional and volumetric data of biological tissues using a laser-interferometric approach. This allows for measurement of morphological parameters in vivo and noninvasively.[1] Although routinely utilized for the assessment of tissue morphology and vascular parameters in various medical fields, its application for the evaluation of neurological parameters is still mostly limited to clinical research and the use of dedicated OCT prototypes.

Optophysiology or optoretinography (ORG) are terms summarizing noninvasive methods to assess stimulus-evoked alterations of optical properties in living tissue called intrinsic optical signals (IOS).[2–5] Intrinsic optical signals in the outer retina are thought to be an objective indicator for photoreceptor function.[6] They have been shown to be altered in certain pathologies and are therefore investigated as biomarker for the early detection of retinal[7–9] and neurological diseases.[10,11]

Studies using OCT to measure IOS report changes in the optical path length (OPL) between various boundaries of the outer retina as well as changes in the backscattering and back-reflecting of certain layers before and

after light stimulation in animal models[12–14] and in human subjects.[7,10,15–18]

Prior studies reported the outer segments of the photoreceptor cells (OS), the retinal pigment epithelium (RPE), and the subretinal space (SRS), that is, the space in between the aforementioned structures, as origins of IOS. A complex homeostasis among the three is the subject of investigation: the SRS has been shown to hydrate in the presence of light stimulation in experimental animal studies using immunohistochemistry,[19] imaging ion-selective microelectrodes,[20–22] or diffusion weighted magnetic resonance imaging.[23] This finding has been confirmed in studies using OCT in mouse models and applying different light stimuli.[24–26] In our prior studies in healthy human volunteers, we found a reduction in rod SRS depth after application of long duration photopigment bleaching light stimuli.[16,17] Previous research using OCT in humans have shown distinct changes in the length of OS associated with a photopigment bleaching exposure. Abramoff and colleagues, based on a similar protocol to ours, reported a decrease of distance between inner segment/outer segment (IS/OS) junction and RPE in healthy subjects,[7] whereas in other studies using different light stimulation – predominantly based on short light flashes – an elongation of photoreceptor OS, was reported.[15,18,27,28] However, the origin of both IOS – elongation of OS or decrease in SRS – might be different physiological effects that depend not only on stimulus duration but also stimulus strength.

Measurement of light or dark adaptation-related IOS in the outer retina might be valuable in a number of diseases. In age-related maculopathy, dark adaptation was shown to be impaired.[29,30] Here, IOS in the outer retina can serve as a biomarker for early changes associated with the development of age-related macular degeneration (AMD). Furthermore, experimental data in mice revealed that oxidative stress impairs the light-dark related hydration of the SRS, which could be used as a biomarker for changes in the outer retina related to diabetic retinopathy.[25] In a previously cited study, Best disease patients during light stimulation revealed a change in OS length, which significantly differed from that in healthy subjects.[7] The development and establishment of methods for measuring IOS based on commercial OCT systems could stimulate research in the field of optophysiology, as the techniques would then be accessible to larger patient groups in a clinical setting.

In the current study, we used our previously reported approach for measuring the outer retinal IOS based on a commercial OCT platform and an OCT signal model in a larger study cohort and explore other potentially confounding factors, like diurnal variations in the outer retinal signal over the course of the day. Further, we performed repeated measurements in the same subjects to test the repeatability of the method.

## Methods

### Human Subjects

IOS in the temporal outer retina were measured in 15 healthy subjects, 5 of which were already included in our previous study[17] performed at the Center for Medical Physics and Biomedical Engineering at the Medical University of Vienna. The study was approved by the local ethics board and the competent authorities and was performed in adherence to the Declaration of Helsinki[31] and to the Good Clinical Practice guidelines. Study participants gave their written informed consent after explanation of the study rationale. All subjects underwent a general medical examination and standard eye examination including perimetry before measurements. Inclusion criteria for the healthy study participants were: age of at least 18 years, normal ophthalmic findings, and ametropy $\leq$3 dpt. Exclusion criteria were: presence of any abnormalities preventing reliable measurements, ocular inflammation and ocular disease interfering with the study aims, use of photosensitizing medication (phototoxic drugs and photoallergic drugs) in the 3 months preceding the study, presence of any condition with the possibility of causing photosensitivity, including systemic lupus erythematosus, Porphyria, Vitiligo, Xeroderma Pigmentosum, and Albinism, ocular surgery in the 3 months preceding the study, and the presence of any form of epilepsy, pregnancy, planned pregnancy, or lactating. To obtain pupil dilation, ensuring that a defined amount of light impinges onto the retina, the study eye received one drop of mydriaticum 0.5% (AGEPHA Pharma s.r.o., Senec, Slovakia). For the diurnal measurements on study day 4, the application was repeated before every third measurement in order to maintain mydriasis.

### OCT Imaging and Analysis

The experimental setup, measurement protocol, data processing, and OCT signal model for peak determination have been described in detail previously.[16,17,32,33] Briefly, a commercial OCT platform (Cirrus 4000; Zeiss Meditec, Jena, Germany) was used to acquire volumetric OCT data of the temporal retina. A comprehensive A-scan average was calculated by registering and averaging all A-scans of the scanned field of view. To estimate the exact location of the outer retinal structures providing the boundaries in the cross-sectional OCT image, a model based on the sum of seven Gaussian curves and slope correction was established.[17] Here, rod outer segment tips (ROST), RPE, choriocapillaris, and choroid were modeled by one curve each, whereas the IS/OS junction complex was represented by three curves, the outermost of which, adjacent to the ROST, was shown to originate from the cone outer segment tips (COST).[17] The external limiting membrane (ELM) was used as the inner reference for determination of the relative peak positions.

OPL in the Results section are given as $d_B^A$, where A and B indicate the corresponding layers and $d$ the distance between them. Relative OPL changes are given as $\Delta d_B^A$, with $\Delta d$ being the change of the distance with respect to the average of the baseline measurements ($t = -10...0$), in the following referred to as "baseline."

In order to assess light adaptation in the outer retina, 10 baseline measurements, each comprising a volumetric data set with a size of 320 × 300 × 1024 voxels covering an area of 3.0 × 2.4 mm$^2$ on the peripheral, temporal retina at an eccentricity of approximately 14 degrees (Fig. 1) were performed in ambient room light and with a pause of 1 minute between them. Then, the measurements were performed after the retina was exposed to a wide field light stimulus, first for 5 minutes and then 9 times for 1 minute in between OCT measurements, resulting in 10 measurements after light stimulation. Lateral stabilization of the acquired volumetric data set on the intended region of interest and consistency of the measurement location at different time points were assured by tracking software implemented in the OCT system and

Investigative Ophthalmology & Visual Science

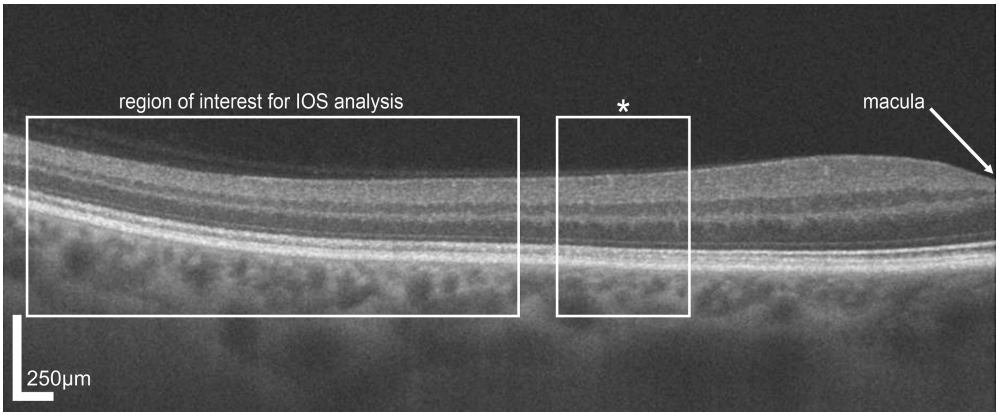


**Figure 1.** Wide-field OCT scan acquired with a commercial OCT system. The image shows the region of the temporal retina at which outer retinal IOS where measured. Hypo- and hyper-reflective bands corresponding to the different retinal layers can be seen. The asterisk indicates the region the cross-sectional image in Figure 2A was taken.

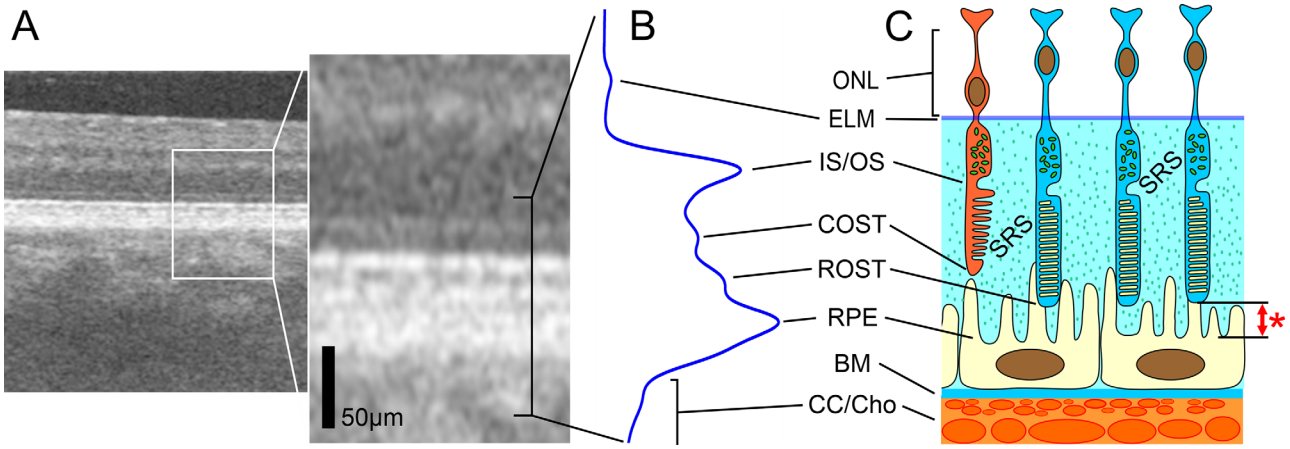


**Figure 2.** Cross-sectional OCT image of the temporal retina and schematic representation of the revealed outer retinal layers. ONL, outer nuclear layer; ELM, external limiting membrane; IS/OS, inner segment/outer segment junction; COST, cone outer segment tips; ROST, rod outer segment tips; RPE, retinal pigment epithelium; BM, Bruch membrane; CC, choriocapillaris; Cho, choroid. The *red asterisk* indicates the SRS OPL assessed in this study. For better visibility of the outer retinal bands, particularly that of the COST, the cross-sectional data was acquired at an eccentricity of approximately 7 degrees.

confirmed retrospectively by the monitoring of landmarks like small vessels in en face projections of the OCT image data sets. Although the SRS, that is, the space in between the distal part of the photoreceptors and between the photoreceptor OS tips and the RPE, is a volumetric structure, when SRS changes are discussed in this manuscript, reference is made to changes in the OPL $d_{RPE}^{ROST}$ (Fig. 2).

## Light Stimulation and Fractional Bleach

Luminance levels were measured with a digital luminance meter (RS-137; RS Components Ltd., Frankfurt/Main, Germany), whereas rod photoreceptor fractional bleach was estimated based on the work of Thomas and Lamb[34] and considering a pupil diameter of 7 mm. Under ambient light conditions, with a luminance of 100 cd/m$^2$ at the laboratory walls, a fraction of 14% rod photopigments was bleached. Light stimulation was realized using a light therapy device (EnergyLight; Philips International B.V., Amsterdam, The Netherlands) providing a luminance of $2 \times 10^4$ cd/m$^2$. The first 5-minute stimulus bleached about 97% rod photopigments, the subsequent 9 stimuli with a duration of 1 minute applied in between OCT measurements led to a fractional bleach >99%. The luminance in the darkened room was approximately 1 cd/m$^2$, which did not lead to bleaching of a significant amount of pigment. When looking into the OCT system during the measurements, the study eye was exposed to a luminance of approximately 20 cd/m$^2$, resulting from both the OCT measuring light and the internal fixation target based on green LEDs, not leading to significant rod photopigment bleaching within the measurement duration of about 20 seconds.

The irradiance of the light therapy device is well below the limit for retinal irradiance, as specified by the standard for light hazard protection.[35]

## Study Days

An adaptation phase of 10 minutes before the beginning of each series of measurements was held to adapt the subject's retina to the lighting conditions in the laboratory.

In total, 4 study days were scheduled. The measuring protocols are summarized in Figure 3. In order to evaluate the repeatability of the IOS assessments, the measurement

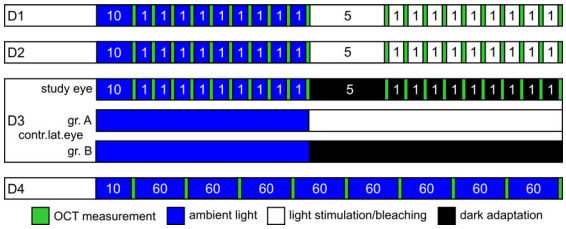


**Figure 3.** Measuring protocol of the different study days. Study days D1 and D2 evaluated the repeatability of light adaptation experiments. On D3, the effect of dark adaptation on outer retinal layers was measured and on D4, diurnal variations of the SRS were investigated.

protocol described in the previous sections was performed in all 15 participants on 2 days (D1 and D2) with a minimum of 2 days between them and at approximately the same time of the day.

The outer retinal OPLs during dark adaptation were measured on study day 3 (D3). Following 10 baseline measurements in ambient light, as on D1 and D2, the study eye was covered using an eye patch and a 1-sided blindfold and only opened for OCT measurements that were performed after an initial 5-minute dark-adaptation period and then within 1-minute intervals and with the room lights switched off. In eight of the subjects, the contralateral eye was stimulated with the white-light stimulus used for light adaptation measurements. Here, we aimed to investigate whether alterations in ocular perfusion that can be induced in both eyes by a stimulus applied only to the contralateral eye, can lead to IOS changes. In the other half of the subjects, the non-measured eye continued without covering in dim room light.

On study day 4 (D4), in order to investigate diurnal variations in the SRS, OCT measurements in ambient room light without stimulation were performed at baseline (T0) in the morning at 8 AM and then every hour on the hour over a period of 8 hours, corresponding to measurements T0, T1, ..., T8. On this study day, all test subjects appeared in the laboratory at the same time and also spent the entire study day indoors in the hospital where ambient light conditions were constant.

### Statistical Analysis

Statistical tests were performed in R Studio (version 1.4.1717) and SPSS (IBM SPSS Statistics 28.0). Continuous variables are given as mean ± standard deviation (SD). The mean OPL $d_{RPE}^{ROST}$ before and during the light stimulation period (D1 and D2) or the dark adaptation period (D3) as well as its changes with respect to the subject's individual baseline were compared using a paired *t*-test per time point. No formal correction for multiple testing was applied due to the explorative character of this study. Comparison of the average baseline values on the first 2 study days was performed using a paired samples *t*-test. For assessment of repeatability, the intraclass correlation coefficient (ICC) for a two-way mixed effects model was calculated for absolute agreement for individual OPL $d_{RPE}^{ROST}$ measurements and for the relative change of single OPL $d_{RPE}^{ROST}$ measurements to subjects' individual baseline between D1 and D2. Furthermore, the mean area under the absolute stimulus response curve (AUC) was calculated for both study days and compared using a paired *t*-test. OPL $d_{RPE}^{ROST}$ changes as measured in the groups of subjects having received light stimulation on the contralateral eye and those who did not, were compared using a Student's *t*-test per time point. For all statistical tests, a *P* value of 0.05 was considered the level of significance.

## Results

### Light Adaptation

The data of 15 healthy Caucasian subjects, whose characteristics are summarized in the Table, were included in the analysis.

In Figure 4, example OCT images and corresponding comprehensive A-scans that reveal the outer retinal depth profile in the measurement region before and during light stimulation are depicted. Comparison of the original tomograms in Figures 4A and 4B reveals only minor differences, that is, a widening of the hyporeflective band between IS/OS junction complex and PRE and a merging of the double-banded structure representing ROST and RPE during light stimulation. OCT images in Figures 3D and 3E show an intermediate post-processing step where each vertical line in the image represents the average of one B-scan in the volumetric image stack. The profiles in Figures 4C and 4F clearly reveal the OPL decrease of the rod SRS, reflected by the convergence of the OCT boundaries of ROST and RPE.

In Figure 5, the relative change of the ROST and RPE peaks during the light stimulation periods on study days D1 and D2 are shown. The average baseline OPL $d_{ROST}^{ELM}$ over all subjects was 62.8 ± 2.2 µm on D1 and 62.1 ± 2.8 µm on D2 ($P = 0.179$). After a cumulative light exposure of 14 minutes, a significant increase $\Delta d_{ROST}^{ELM}$ by 3.4 ± 2.8% to a mean OPL of 64.9 ± 3.0 µm ($P < 0.001$) on D1 and by 3.7 ± 2.8% to 64.3 ± 3.3 µm ($P < 0.001$) on D2 ($P = 0.62$ for study day comparison) was observed. The average OPL $d_{RPE}^{ELM}$ on D1 and D2 at baseline were 73.5 ± 2.4 µm and 72.4 ± 3.1 µm, respectively ($P = 0.112$). During light stimulation, this distance decreased by 2.8 ± 1.6% to a value of 71.4 ± 2.6 µm ($P < 0.001$) on D1 and by 2.7 ± 1.9% to 70.4 ± 2.5 µm ($P < 0.001$) on D2 ($P = 0.319$ for study day comparison). These minimum values were observed after cumulative stimulation times of 9 and 10 minutes on D1 and D2, respectively.

Based on the data depicted in Figure 5, the OPL change $\Delta d_{RPE}^{ROST}$ of the rod SRS during light stimulation was calculated and is depicted in Figures 6A and 6B.

The mean baselines rod SRS of all subjects during ambient light condition did not show a statistically significant difference between D1 and D2 with $d_{RPE}^{ROST}$ being 10.7 ± 1.4 µm and 10.4 ± 1.5 µm ($P = 0.192$), respectively. During light stimulation, the rods SRS decreased by 21.3 ± 7.6% and 19.8 ± 8.5% ($P = 0.361$ for study day comparison),

**Table.** Characteristics of Subjects and Studied Eyes

| | $n = 15$ |
|---|---|
| **Age, y** | 30 ± 6 |
| **Gender (M/F)** | 6/9 |
| **Best corrected visual acuity (ETDRS letters)** | 85 ± 3.8 |
| **Dioptric power (dpt)** | 0.3 ± 1.1 |

Data are given as mean ± SD.
ETDRS, Early Treatment Diabetic Retinopathy Study.

Investigative Ophthalmology & Visual Science

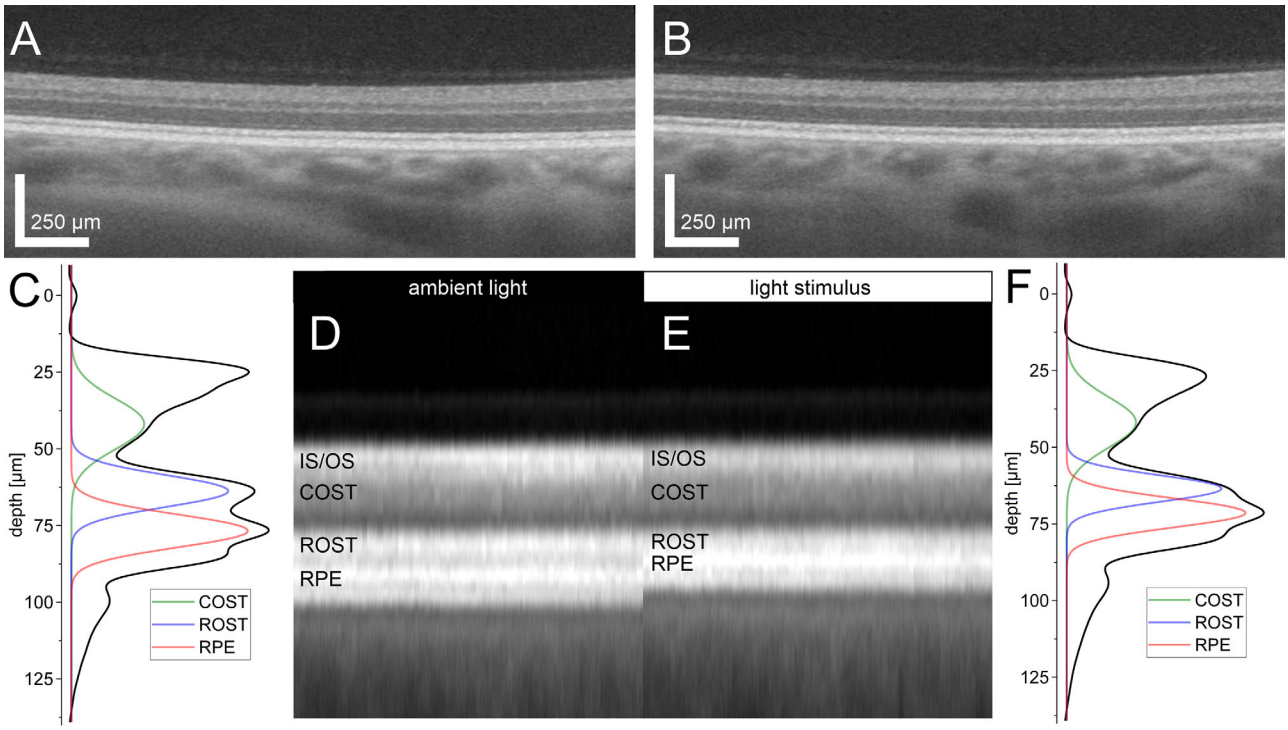


**Figure 4.** IOS imaging in the temporal outer retina before and during light stimulation. Cross-sectional images acquired at (**A**) baseline and during (**B**) light stimulation reveal hyperreflective outer retinal bands of IS/OS junction, ROST, and RPE. (**D, E**) preprocessed OCT images show the average of the volumetric data along the fast axis, that is, one column in the images represents one B-scan of the acquired volumetric data set. Comprehensive A-scans (**C**) before and (**F**) during stimulation with white light reveal the decrease of the SRS OPL in the bleaching condition.

respectively, reaching its minimum after a cumulative stimulation time of 12 minutes on both days. Here, OPL $d_{RPE}^{ROST}$ was significantly smaller in comparison to the baseline at all time points on both study days. The results of this analysis are summarized in Supplementary Tables S1 and S2 in the supplementary materials. In all subjects, a significant difference between baseline SRS and SRS during stimulation was found on D1 and on D2 (see Supplementary Tables S3, S4).

Test-retest reliability for the rod SRS measurements, that is, comparison of OPL $d_{RPE}^{ROST}$ of subject i, time point j on D1 with that of subject i, time point j on D2, was good, with ICCs of 0.808 and 0.894 (both $P < 0.001$) for single and average measures, respectively. The mean absolute difference between corresponding measurements was 0.3 ± 1.0 µm (minimum = 0.0 µm and maximum = 3.0 µm). The test-retest reliability for the average change $\Delta d_{RPE}^{ROST}$ during light stimulation relative to individual subjects' baseline was moderate with ICCs of 0.595 (95% CI = 0.137, 0.843) and 0.746 (95% CI = 0.241, 0.915, $P < 0.001$) for single and average measures, respectively. Test-retest reliability of the maximum change of an individual subject was moderate for single measures (ICC = 0.730, 95% CI = 0.376, 0.900, $P < 0.001$) and good for average measures (ICC = 0.844, 95% CI = 0.546, 0.947, $P < 0.001$). The mean differences for all subjects between the corresponding rod SRS light responses on D1 and D2 was 0.6 ± 0.5 µm (average change) and 0.7 ± 0.5 µm (maximum change), each with no significant difference between the two study days. The AUCs based on the data depicted in Figure 7 were 14.8 ± 9.4 µm × minutes and 15.5 ± 7.5 µm × minutes for D1 and D2, respectively, with no significant difference between study days ($P = 0.782$).

## Dark Adaptation

The mean baseline OPL of the rod SRS during ambient light condition on D3 was 10.3 ± 1.4 µm. After dark adaptation of the study eye, the SRS increased in both groups, those with exposure to white light and those exposed to ambient light in the contralateral eye. Significant differences versus baseline were found after an initial dark period of 5 minutes and subsequent 4 one-minute intervals (Supplementary Table S5, Fig. 8) in both groups. The maxima of 11.2 ± 1.4 µm (contralateral white light stimulation) and 11.0 ± 1.7 µm (contralateral ambient light) were reached after 7 cumulative minutes of intermittent dark adaptation ($P = 0.945$ for group comparison). No significant differences were found between the mean changes versus baseline at the different time points for the subjects who did receive light stimulation on the contralateral eye versus those who did not ($P = 0.219...0.9994$; see Fig. 8C). Beyond 7 minutes of dark adaptation, the rod SRS OPL revealed a slow decrease returning to values with no significant difference to baseline (paired *t*-test), even though dark adaptation was continued in between measurements.

## Diurnal Variations of the SRS

In the measurements over 8 hours on D4, the subject average of the rods SRS over all time points was 9.6 ± 1.2 µm. The averages of individual subject's maxima and minima were 10.2 ± 1.2 µm and 9.0 ± 1.2 µm with mean deviations from individual subject's average of +6.6% and −5.7%, respectively. The lowest mean values for the SRS were observed

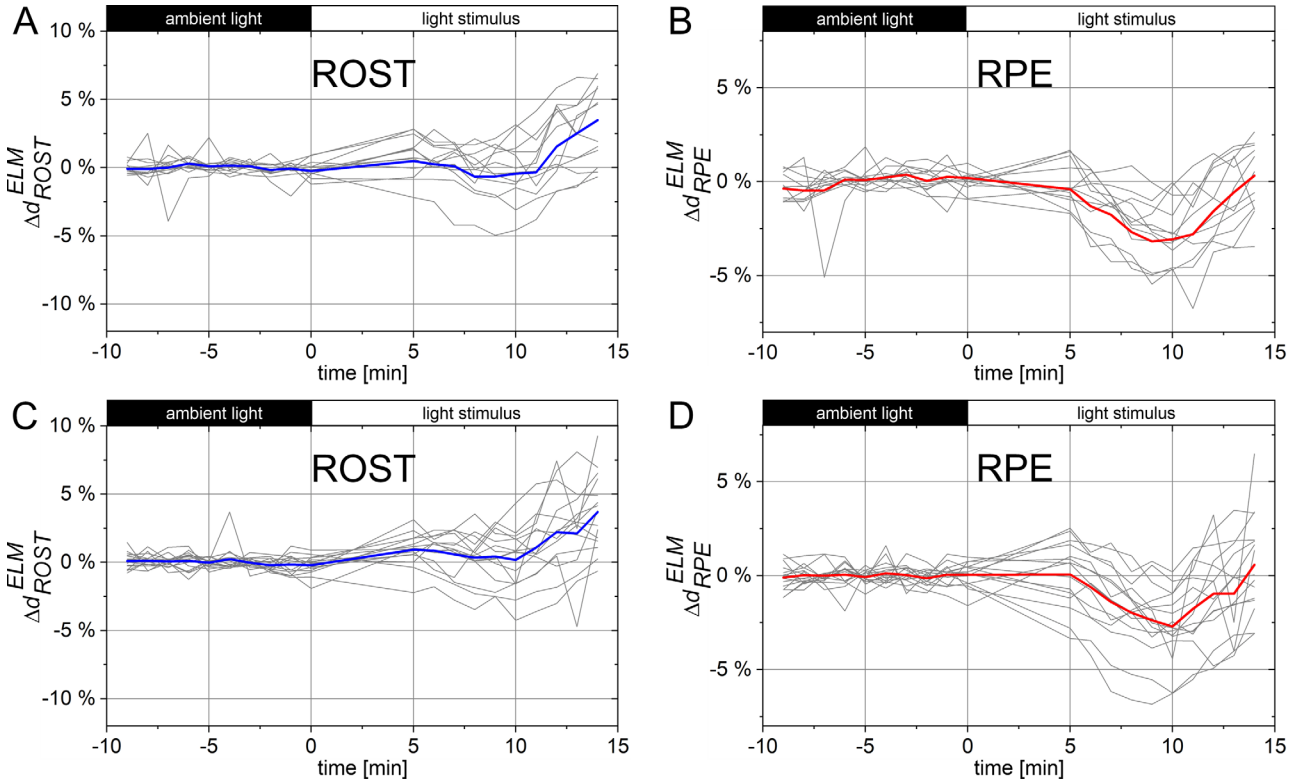


**Figure 5.** OPL changes $\Delta d_B^{ELM}$ relative to the baseline for the fitted Gaussian peaks attributed to the ROST and the RPE measured on (**A**, **B**) D1 and (**C**, **D**) D2. The average of all subjects is given as a *bold*, *colored line*, values of individual subjects are represented by the *grey lines*. The time axis represents the measurement time relative to the stimulation onset. The stimulation period started directly after the last measurement in ambient room light. Linear interpolation was performed between measurement time points.

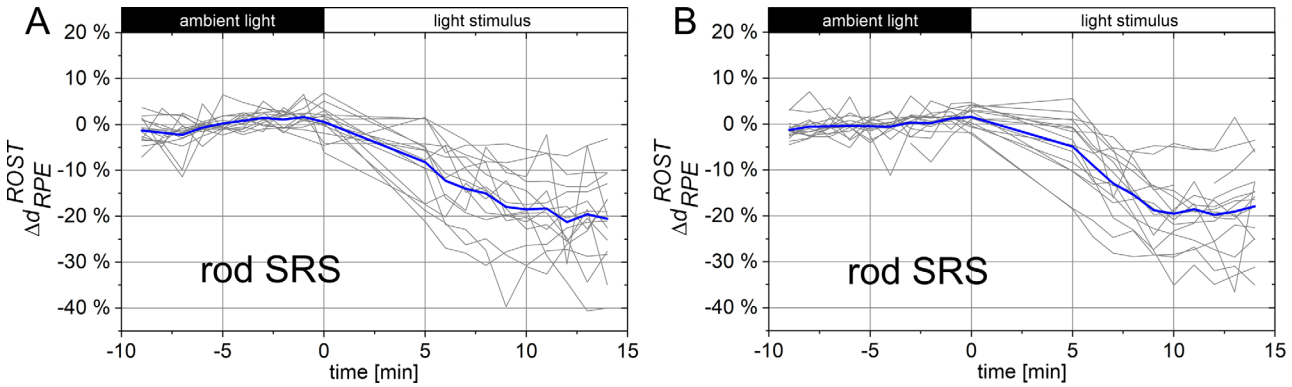


**Figure 6.** Repeatability of light adaptation assessment on (**A**) D1 and (**B**) D2. Changes of the rod SRS, that is, the OPL between ROST and PRE, relative to the baseline in ambient light. The average of all subjects is given as a *bold*, *colored line*, values of individual subjects are represented by the *grey lines*. The time axis represents the measurement time relative to the stimulation onset. The stimulation period started directly after the last measurement in ambient room light. Linear interpolation was performed between measurement time points.

in the first (T0) and in the last (T8) measurements with mean deviations of −2.2% and −1% from subject average, respectively. Measurements performed at time points T2, T3, T4, and T5 revealed subject averages 1.5%, 1,1%, 0.3%, and 1.8% larger than the average over all time points. None of these mean deviations from subjects' average reached statistical significance. The smallest and largest variations of the SRS OPL in an individual subject were 0.4 µm and 2.83 µm, respectively. The time course over the measurement period is shown in Figure 9 both for the individual subjects and for the average from their data.

## Discussion

In the present study, the use of a commercial OCT platform and a dedicated signal model to assess IOS in the outer retina were tested for their reproducibility in a healthy study population. The focus was on the SRS, that is, the space between

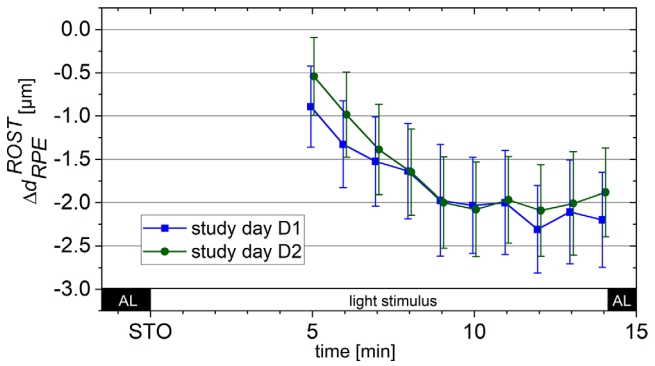


**Figure 7.** OPL change of the rod SRS during light adaptation on D1 and D2. Plots show the average changes $\Delta d_{RPE}^{ROST}$ of all subjects and the 95% confidence intervals at each day. The time axis represents the measurement time relative to the stimulation onset. Linear interpolation was performed between measurement time points. AL, ambient light; STO, stimulus onset.

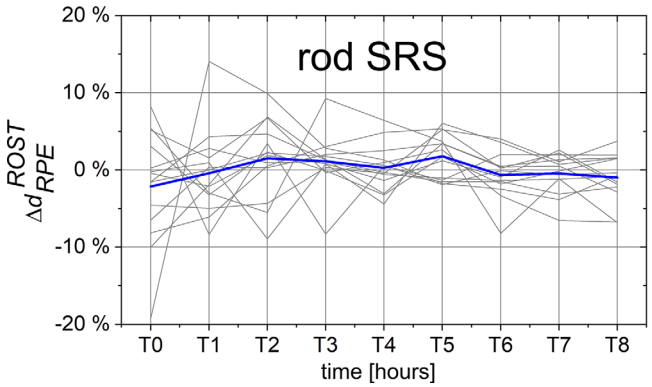


**Figure 9.** Diurnal variations of the rod SRS. OCT measurements were performed in ambient room light without stimulation at baseline (T0) in the morning at 8 am and then every hour on the hour over a period of 8 hours. The average subject deviation from baseline is given as a *bold*, *blue line*, values of individual subjects are represented by the *narrow lines*. Linear interpolation was performed between measurement time points.

ROST and RPE at an eccentricity in which rod photoreceptors dominate.

A long duration light stimulus led to a decrease of the rod SRS by approximately 20%, attributable to position changes of the OCT boundaries of ROST and RPE. An interesting feature is the relatively long time after stimulus onset that it takes for the ROST position to change relative to the ELM. Only after 10 minutes total stimulation time, an increase of $d_{ROST}^{ELM}$ was observed. In contrast, $d_{RPE}^{ELM}$ revealed a significant decrease after just 6 minutes cumulative stimulation and reached its minimum after 9 to 10 minutes. Thereafter, the band position approached the baseline again, despite continuation of stimulation. A similar time course as ours was reported by Lu and co-workers for the OPL $d_{RPE}^{IS/OS}$ after flash exposure of dark-adapted heathy subjects.[27] Here, after an initial increase, the OPL reached its minimum at 10 to 15 minutes before the response curve oscillated back toward the baseline. We could not show the first increase of the OPL between our internal reference ELM and the RPE band

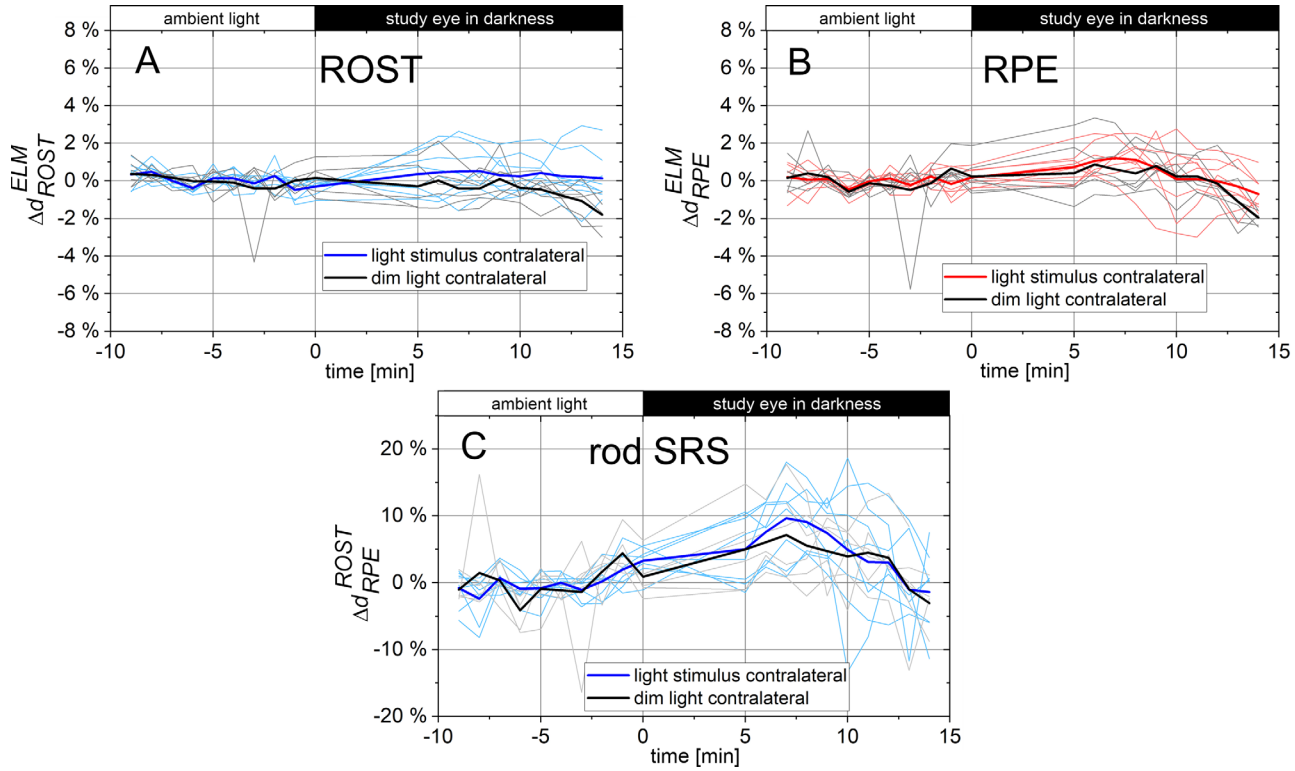


**Figure 8.** Optical path length of the rod SRS during dark adaptation. The averages of all subjects of a group are given as *bold lines*, values of individual subjects are represented by the *narrow lines*. The time axis represents the measurement time relative to the stimulation onset. The darkness period started directly after the last measurement in ambient room light. Linear interpolation was performed between measurement time points.

Investigative Ophthalmology & Visual Science

due to the long first stimulation phase in our experiments. Therefore, only the subsequent decrease during light adaptation was revealed. However, in this comparison, it must be emphasized that, in the previously cited study, the time courses after a flash stimulus were examined, whereas in the present experiments the stimulus was continued intermittently between measurements leading to rod photopigment bleaching. Our findings are consistent with a study by Abramoff and colleagues who – using a long stimulus – reported a significant decrease of the OPL $d_{RPE}^{IS/OS}$.[7] Although the qualitative signal responses of all studies are similar, a direct quantitative comparison, particularly of the relative OPL changes, should be treated with caution, as we did not use the IS/OS junction but the ELM as reference for our band position analysis. Noteworthy are also the results presented by Azimipour and colleagues who investigated single rod and cone photoreceptors in humans before and after stimulation with a 10 ms flash that bleached 4% photopigment employing a synchronized scanning light ophthalmoscopy (SLO) and adaptive optics (AO) OCT system.[18] Authors demonstrated a splitting of the RPE band along with a convergence of one of the bands to the ROST taking place over a time interval of a few seconds and appearing to be similar to our observation where the hyper-reflective bands of ROST and COST merge during light stimulation.

When investigating the origin of IOS, different mechanisms with different time frames leading to both fast (milliseconds to seconds) and slow (minutes to hours) changes in the OCT signal, have to be considered.[36] Slow IOS that correspond to volume changes of the SRS, in the current study, reflected by changes in $d_{RPE}^{ROST}$, were linked to mitochondria-driven water-movement in the outer retina.[36,37] Here, the hydration of the SRS is regulated by the RPE fluid transporter activity according to the energy requirement of the retina in the different adaptation states. During long light exposure and when light intensity reaches levels leading to bleaching of a significant fraction of the photopigment, the translocation of signaling proteins[38] should be taken into account. The translocation of transducin from the OS to the IS requires light intensities that are saturating for rods[39] – as in the present study where > 99% of rod photopigments are bleached – happens on a time scale of tens of minutes[40] and serves the adjustment of the energy consumption in the phototransduction cascade while also having a neuroprotective aspect.[38,41] However, if this process plays a role in the change of SRS volume when the full fraction of rod photopigment is bleached has yet to be elucidated. A third physiological factor possibly contributing to the IOS is the light-driven melanosome movement into the apical processes of the RPE cells, which is a means to alter visual sensitivity and has been demonstrated in different species.[42–46] Optical imaging modalities like Raman spectroscopy,[47] photoacoustic,[48] or two-photon microscopy[49,50] allow for in vivo assessment of melanin both in the skin and in the retina. However, due to the small numerical aperture of the human eye, limitations regarding the achievable depth of field – and thus the resolution to visualize potential changes in axial position – hamper an application in the human retina and investigation of melanosome movement within the RPE. Because in the current study, in the first phase of light stimulation the SRS change is solely caused by a displacement of the RPE band, we assume that the initial decrease in rod SRS is caused by a reduction in SRS hydration as a result of upregulation of RPE fluid transporter activity for waste water removal. Here, also volume changes in the RPE apical microvilli that affect the SRS volume may play a role. The later increase in $d_{ROST}^{ELM}$ could be indicative for an elongation or increase in volume of the OS.

An important criterion when examining the stimulation response is the adaptation state of the retina before stimulus application. In the current study, the retina was adapted to the ambient light. The following light stimulations with $2 \times 10^4$ cd/m$^2$ luminance led to bleached fraction >99% and a decrease in the SRS OPL. In mice, a stimulus with $1 \times 10^4$ cd/m$^2$ luminance and 80 seconds duration caused a significant increase of the $d_{RPE}^{ELM}$, associated with an increase in SRS OPL, when the retina was fully dark-adapted at baseline.[36] Interestingly, no significant change of this distance was found for light-adapted mice receiving this stimulus. On the other hand, when comparing the ground states – light-adapted versus dark-adapted – the same authors found an approximately 10% larger OPL $d_{RPE}^{ELM}$ for the light-adapted state. Thus, it is reasonable to analyze light adaptation from two perspectives: one is the adaptation state, that is, to which light intensity the retina is currently adapted. The other is the dynamic process, characterized by the "direction" in which the light adaptation changes, that is, from lighter to darker or vice versa. This point seems particularly important when looking at the results of study day 3. Here, the influence of dark adaptation on the rod SRS was evaluated. Due to the covering with an eye patch between the measurements, the retina of the study eye is in dark-adapted state (luminance 0 cd/m$^2$). When the eye patch was removed for the measurement, the retina was exposed to both the dimmed room light and the OCT measurement light (20 cd/m$^2$), which means that it was actually in the process of light adaptation at the moment of measurement, where then an increase of the rod SRS as compared to the baseline was observed. The time span between removing of the eye patch and beginning the measurement was about 15 seconds. After the initial dark period of 5 minutes as well as after the subsequent 2 one-minute dark intervals, an increase of the rod SRS as compared to the baseline performed in ambient light (100 cd/m$^2$) was observed. As expected, lighting conditions in the contralateral eye had no influence on the measured IOS. The main difference of this light adaptation processes as compared to the first 2 study days is the luminance level that the retina is adapting to, on day 3 not resulting in bleaching of rod photopigment. This makes the translocation of signaling proteins occurring at high light intensity very unlikely and could lead to mitochondria-driven water movement as initiated by the phototransduction process being the main cause of the observed IOS. If dark adaptation status were the origin of the IOS, the observed increase in SRS OPL would most likely be the opposite of what has been reported in experiments in mice, where minute-long dark adaptation intervals resulted in a significant decrease in $d_{RPE}^{ELM}$[13] or OS equivalent length.[12] However, it must be emphasized that different IOS were measured: solely the SRS in our study, distances that include the IS, OS, and SRS or the OS and SRS in the experiments performed by the other authors. If, on the other hand, the SRS changes were related to the process of light adaptation, the OPL increase would be consistent with previous reports on both dark-light transition[12] and light stimulus after dark adaptation,[27,36] the latter associated with bleaching of a fraction of rod photopigment. However, the interpretation is complicated by the baseline condition the SRS change is related to as this data was recorded under ambient light (100 cd/m$^2$) but inevitably while looking into the OCT (20 cd/m$^2$). This aspect underscores the

general challenge of measuring the effect of dark adaptation, where not only the ambient light conditions but also the luminance emanating from the measurement system, that at typical OCT wavelength can be perceived, must be considered. Here, when evaluating light adaptation states, the lighting conditions provided by the instrument might alter the state to be measured by initiating an adaptation process. In the current experiments, the initial increase of the SRS in the dark/dim phase after complete darkness could have been caused by the process of light adaptation. Because of the relatively short, repeated dark adaptation intervals, the time available to establish a dark-adapted state from which the process of light adaptation would start again was too short, so that the SRS OPL subsequently approached baseline. Therefore, if aiming to measure adaptational IOS based on commercial OCT platforms, it seems more feasible to assess transitions between dim/ambient to brighter lighting conditions or vice versa as a state of complete dark adaptation is difficult to maintain until the measurement. Interestingly, two studies assessing the effect of prolonged dark adaptation in healthy human subjects based on commercial OCT systems did not find any significant thickness difference between light- and dark-adapted retina.[51,52] Su and colleagues attributed this discrepancy between their and previous studies in mice[12,13,53,54] to homeostatic processes, where after full adjustment to the new lighting conditions, the retinal ATP consumption might return to baseline level.[52] Another study in humans reported the hyporeflective band between RPE and ROST to increase in magnitude already after a 2-minute period of dark adaptation.[10,53] These findings indicate that even short periods of dark adaptation lead to outer retinal changes.

Analysis of the test-retest reliability of the rod SRS data based on the identical study days D1 and D2 showed a good reproducibility of the results. The significant decrease of the rod SRS during light adaptation could be revealed in all subjects and both study days. This together with the very similar time course of the stimulus response on both study days and the good agreement of the maximum SRS OPL change of the individual subjects, indicate that physiological processes driven by the light stimulus are reproducibly measurable. The rather large range of the stimulus response of individual subjects might have been caused by individual differences in light sensitivity, which, for example, is influenced by the pigmentation of the fundus, and also individual differences in light recovery, because, in the current approach, due to the external stimulation, the IOS are measured shortly after stimulus application. Therefore, future studies in both an elderly population and, more importantly, patients suffering diseases affecting photoreceptor function are needed to investigate the potential of the presented approach to discriminate between healthy and diseased eyes based on the given measurement accuracy and variability. As previous studies have shown outer retinal IOS in patients to alter both regarding their direction of change versus baseline[7] and their amplitude[55] when compared to a healthy population, only these additional studies can show in which disease pattern the approach possesses discriminatory capabilities demonstrating the rod SRS as a valuable biomarker. These studies should take into account both the limitations and potential adaptation that will be discussed in a later section.

Measurements of the average rod SRS performed at nine time points throughout the day revealed variations in the order of approximately six percent in both positive and negative directions. However, no distinct time course of the OPL was observed and none of the diurnal alterations reached a statistically significant difference from the average of all subjects. This seems surprising at first sight because different OCT studies in both humans[56,57] and mice[58] have shown photoreceptor OS OPL changes that were associated with circadian regulation,[59] photoreceptor OS phagocytosis by the RPE and diurnal renewal. The main difference to our study is, first, the type of photoreceptors measured – rods in ours, cones in the previous studies – and the type of the measurement system. Reports using AO-OCT allow for resolution of individual cone photoreceptors thus providing a very high SNR and sensitivity for detection of positional changes of the morphological landmarks in the OCT data. In contrast, due to the averaging of the volumetric data in the present study and due to the fact that this renewal process does not happen perfectly synchronized for all photoreceptors at one point in time, small changes might have been masked by the averaging process and the resulting peak broadening in our data. The observed alterations of the rod SRS in individual subjects might have been due to different positioning of the head in the headrest and resulting angle of incidence alterations of the probe beam onto the retina. This factor was minimized by adjusting the SLO image of the current measurement to the initial recording based on vessel landmarks and further aligning the incidence point of the probe beam onto the pupil. It is obvious that with the observed variations in individual subjects' SRS, the approach in its current form is not suitable for examining diurnal changes in the absolute SRS OPL or to draw conclusions from inter-session changes of this IOS. However, their influence on the assessment of a stimulus response within a measurement session is small as their magnitudes are smaller than the SRS OPL changes observed after light stimulation. This is further supported by the small variance in the baseline measurement on study days D1, D2, and D3 performed with shorter time intervals between measurements.

The employed OCT signal model also revealed a peak that corresponds with high probability to the position of the COST in the comprehensive A-scan. However, due to the lower signal-to-noise-ratio (SNR) of the signal in the peripheral retina, accuracy of the peak detection is lower. Therefore, changes of the cone SRS, that is, the OPL $d_{RPE}^{COST}$, were not further investigated.

The measurement of IOS in the human outer retina has been subject of increased research in the last years and a number of studies have shown the potential of OCT[5,14,15,27,53] and its technical extensions[56,57,60] for the detection of such signals. The ultimate goal is the establishment of noninvasive biomarkers to characterize photoreceptor function allowing both the early detection of disease-related changes and the monitoring of treatment. This is of particular importance in retinal diseases like AMD[61,62] where treatment can slow down but not stop or reverse progression. In a recent report, Borelli and colleagues showed that dark adaptation as assessed via OCT is altered in patients with AMD with reticular pseudodrusen.[55] Assessment of the hydration of the SRS and its regulation, as in the study presented here, can provide a biomarker for the functionality of RPE cells as it is well known that age-related changes in the RPE layer play a major role in the development of AMD.[63,64]

The use of commercial OCT systems, as in the aforementioned and also our study, might easier facilitate the transfer

of IOS assessment into clinical practice. To render possible, however, we must first investigate how the light-induced SRS changes measured here in healthy subjects differ from those in patients, both in terms of the presence and extent of a stimulus response and its time course.

The present study has some limitations that are worth mentioning. First of all, only young subjects were measured. This was done in an effort to investigate the stimulus protocol, the repeatability, and to identify limitations of the current approach based on a study population, that due to their good fixation abilities, is expected to provide a high data quality. However, as mentioned before, additional studies are needed to demonstrate the clinical utility of the rod SRS IOS driven by photopigment bleaching. In addition, the current stimulus protocol is relatively time-consuming, which could be particularly cumbersome for older subjects and patients. We need to investigate whether, instead of a time course with repeated measurements, simply the maximum stimulus response, that occurred in our subjects after a stimulation period of 12 minutes is sufficient as biomarker for the outer retinal response during bleaching. Furthermore, the current experiment uses a repeated stimulus with OCT measurements in between, which on the one hand could mean that due to the short time interval between them both, not the maximum IOS is measured and, furthermore, a repositioning of the eye before imaging is required. This relatively simple approach was chosen so that the experiments presented here can be implemented for any commercial OCT without any technical effort. Coupling the stimulation light directly into the OCT beam path, for example, via a dichroic mirror in front of the ophthalmic lens of the system, would make measurement during stimulation/bleaching possible even with a higher temporal sampling rate. This would allow a more accurate assessment of the light adaptation process during rod photopigment bleaching and might also help minimize the intersubject variability in IOS magnitude caused by individual differences in the time course of the stimulus response.

In summary, we were able to measure SRS changes that we related to light and dark adaptation of rod photoreceptors with a commercial OCT platform. Analysis of the test-retest reliability showed good repeatability. The findings indicate on the one hand the potential of commercial OCT in measuring slow IOS in the outer retina but on the other hand underline the importance of the precise analysis of the underlying lighting conditions. If the discriminatory capabilities of the current approach can be proven in patient measurements, the method could serve as an easily implementable clinical tool for the early detection of diseases affecting photoreceptor health.

## *Acknowledgments*

Support by Daniela Boryshchuk and Robin Ristl from the Section of Medical Statistics and Angelika Unterhuber from the Center for Medical Physics and Biomedical Engineering at the Medical University of Vienna is gratefully acknowledged.

Funded by the Vienna Science and Technology Fund (WWTF) [10.47379/LS14067].

Disclosure: **A. Messner**, None; **V. Aranha dos Santos**, None; **S. Puchner**, None; **H. Stegmann**, None; **A. Schlatter**, None; **D. Schmidl**, None; **R. Leitgeb**, None; **L. Schmetterer**, None; **R.M. Werkmeister**; None

## *References*

1. Drexler W, Fujimoto JG. *Optical Coherence Tomography*. Berlin Heidelberg New York: Springer International Publishing; 2015:2571.
2. Bizheva K, Pflug R, Hermann B, et al. Optophysiology: depth-resolved probing of retinal physiology with functional ultrahigh-resolution optical coherence tomography. *Proc Natl Acad Sci USA*. 2006;103:5066–5071.
3. Srinivasan VJ, Wojtkowski M, Fujimoto JG, Duker JS. In vivo measurement of retinal physiology with high-speed ultrahigh-resolution optical coherence tomography. *Opt Lett*. 2006;31:2308–2310.
4. Mulligan JB, MacLeod DI, Statler IC. In search of an optoretinogram. *NASA Tech Rep 20010045533*: NASA; 1994.
5. Kim TH, Ma G, Son T, Yao X. Functional optical coherence tomography for intrinsic signal optoretinography: recent developments and deployment challenges. *Front Med (Lausanne)*. 2022;9:864824.
6. Yao X, Wang B. Intrinsic optical signal imaging of retinal physiology: a review. *J Biomed Opt*. 2015;20:090901.
7. Abramoff MD, Mullins RF, Lee K, et al. Human photoreceptor outer segments shorten during light adaptation. *Invest Ophthalmol Vis Sci*. 2013;54:3721–3728.
8. Owsley C, McGwin G, Jr., Clark ME, et al. Delayed rod-mediated dark adaptation is a functional biomarker for incident early age-related macular degeneration. *Ophthalmology*. 2016;123:344–351.
9. Lassoued A, Zhang F, Kurokawa K, et al. Cone photoreceptor dysfunction in retinitis pigmentosa revealed by optoretinography. *Proc Natl Acad Sci USA*. 2021;118. (Online print only).
10. Bissig D, Zhou CG, Le V, Bernard JT. Optical coherence tomography reveals light-dependent retinal responses in Alzheimer's disease. *Neuroimage*. 2020;219:117022.
11. Snyder PJ, Alber J, Alt C, et al. Retinal imaging in Alzheimer's and neurodegenerative diseases. *Alzheimers Dement*. 2021;17:103–111.
12. Li Y, Fariss RN, Qian JW, Cohen ED, Qian H. Light-induced thickening of photoreceptor outer segment layer detected by ultra-high resolution OCT imaging. *Invest Ophthalmol Vis Sci*. 2016;57:OCT105–OCT111.
13. Kim TH, Ding J, Yao X. Intrinsic signal optoretinography of dark adaptation kinetics. *Sci Rep*. 2022;12:2475.
14. Zhang PF, Zawadzki RJ, Goswami M, et al. In vivo optophysiology reveals that G-protein activation triggers osmotic swelling and increased light scattering of rod photoreceptors. *Proc Natl Acad Sci USA*. 2017;114:E2937–E2946.
15. Hillmann D, Spahr H, Pfaffle C, Sudkamp H, Franke G, Huttmann G. In vivo optical imaging of physiological responses to photostimulation in human photoreceptors. *Proc Natl Acad Sci USA*. 2016;113:13138–13143.
16. Messner A, Werkmeister RM, Seidel G, Stegmann H, Schmetterer L, Aranha Dos Santos V. Light-induced changes of the subretinal space of the temporal retina observed via optical coherence tomography. *Sci Rep*. 2019;9:13632.
17. Messner A, Aranha Dos Santos V, Stegmann H, et al. Quantification of intrinsic optical signals in the outer human retina using optical coherence tomography. *Ann N Y Acad Sci*. 2021;1510(1):145–157.
18. Azimipour M, Valente D, Vienola KV, Werner JS, Zawadzki RJ, Jonnal RS. Optoretinogram: optical measurement of human cone and rod photoreceptor responses to light. *Opt Lett*. 2020;45:4658–4661.
19. Uehara F, Matthes MT, Yasumura D, LaVail MM. Light-evoked changes in the interphotoreceptor matrix. *Science*. 1990;248:1633–1636.

20. Huang B, Karwoski CJ. Light-evoked expansion of subretinal space volume in the retina of the frog. *J Neurosci*. 1992;12:4243–4252.
21. Li JD, Gallemore RP, Dmitriev A, Steinberg RH. Light-dependent hydration of the space surrounding photoreceptors in chick retina. *Invest Ophthalmol Vis Sci*. 1994;35:2700–2711.
22. Li JD, Govardovskii VI, Steinberg RH. Light-dependent hydration of the space surrounding photoreceptors in the cat retina. *Vis Neurosci*. 1994;11:743–752.
23. Bissig D, Berkowitz BA. Light-dependent changes in outer retinal water diffusion in rats in vivo. *Mol Vis*. 2012;18:2561–xxx.
24. Berkowitz BA, Grady EM, Khetarpal N, Patel A, Roberts R. Oxidative stress and light-evoked responses of the posterior segment in a mouse model of diabetic retinopathy. *Invest Ophthalmol Vis Sci*. 2015;56:606–615.
25. Berkowitz BA. Preventing diabetic retinopathy by mitigating subretinal space oxidative stress in vivo. *Vis Neurosci*. 2020;37:E002.
26. Zawadzki RJ, Zhang PF, Meleppat RK, Manna SK, Pugh EN. Light induced water movement in the outer retina investigated by optical coherence tomography. *Invest Ophthalmol Vis Sci*. 2019;60:1294.
27. Lu CD, Lee B, Schottenhamml J, Maier A, Pugh EN, Jr., Fujimoto JG. Photoreceptor layer thickness changes during dark adaptation observed with ultrahigh-resolution optical coherence tomography. *Invest Ophthalmol Vis Sci*. 2017;58:4632–4643.
28. Azimipour M, Migacz JV, Zawadzki RJ, Werner JS, Jonnal RS. Functional retinal imaging using adaptive optics swept-source OCT at 1.6 MHz. *Optica*. 2019;6:300–303.
29. Owsley C, McGwin G, Jr., Jackson GR, Kallies K, Clark M. Cone- and rod-mediated dark adaptation impairment in age-related maculopathy. *Ophthalmology*. 2007;114:1728–1735.
30. Steinmetz RL, Haimovici R, Jubb C, Fitzke FW, Bird AC. Symptomatic abnormalities of dark adaptation in patients with age-related Bruch's membrane change. *Br J Ophthalmol*. 1993;77:549–554.
31. World Medical Association. World Medical Association Declaration of Helsinki: ethical principles for medical research involving human subjects. *JAMA*. 2013;310:2191–2194.
32. Dos Santos VA, Schmetterer L, Triggs GJ, et al. Super-resolved thickness maps of thin film phantoms and in vivo visualization of tear film lipid layer using OCT. *Biomed Opt Express*. 2016;7:2650–2670.
33. Aranha Dos Santos V, Schmetterer L, Groschl M, et al. In vivo tear film thickness measurement and tear film dynamics visualization using spectral domain optical coherence tomography. *Opt Express*. 2015;23:21043–21063.
34. Thomas MM, Lamb TD. Light adaptation and dark adaptation of human rod photoreceptors measured from the a-wave of the electroretinogram. *J Physiol*. 1999;518(Pt 2):479–496.
35. International Organization for Standardization (ISO). ISO 15004-2, Ophthalmic instruments — Fundamental requirements and test methods — Part 2: Light hazard protection (ISO/DIS 15004-2:2023). 2023.
36. Gao S, Zeng Y, Li Y, Cohen ED, Berkowitz BA, Qian H. Fast and slow light-induced changes in murine outer retina optical coherence tomography: complementary high spatial resolution functional biomarkers. *PNAS Nexus*. 2022;1:pgac208.
37. Berkowitz BA, Qian H. OCT imaging of rod mitochondrial respiration in vivo. *Exp Biol Med (Maywood)*. 2021;246:2151–2158.
38. Arshavsky VY, Burns ME. Photoreceptor signaling: supporting vision across a wide range of light intensities. *J Biol Chem*. 2012;287:1620–1626.
39. Calvert PD, Strissel KJ, Schiesser WE, Pugh EN, Jr., Arshavsky VY. Light-driven translocation of signaling proteins in vertebrate photoreceptors. *Trends Cell Biol*. 2006;16:560–568.
40. Sokolov M, Lyubarsky AL, Strissel KJ, et al. Massive light-driven translocation of transducin between the two major compartments of rod cells: a novel mechanism of light adaptation. *Neuron*. 2002;34:95–106.
41. Burns ME, Arshavsky VY. Beyond counting photons: trials and trends in vertebrate visual transduction. *Neuron*. 2005;48:387–401.
42. Pang SF, Yew DT, Tsui HW. Photomechanical changes in the retina and choroid of guinea pigs, Cavia porcellus. *Neurosci Lett*. 1978;10:221–224.
43. Zhang QX, Lu RW, Messinger JD, Curcio CA, Guarcello V, Yao XC. In vivo optical coherence tomography of light-driven melanosome translocation in retinal pigment epithelium. *Sci Rep*. 2013;3:2644.
44. Futter CE, Ramalho JS, Jaissle GB, Seeliger MW, Seabra MC. The role of Rab27a in the regulation of melanosome distribution within retinal pigment epithelial cells. *Mol Biol Cell*. 2004;15:2264–2275.
45. Burgoyne T, O'Connor MN, Seabra MC, Cutler DF, Futter CE. Regulation of melanosome number, shape and movement in the zebrafish retinal pigment epithelium by OA1 and PMEL. *J Cell Sci*. 2015;128:1400–1407.
46. Burnside B. Light and circadian regulation of retinomotor movement. *Prog Brain Res*. 2001;131:477–485.
47. Yakimov BP, Shirshin EA, Schleusener J, Allenova AS, Fadeev VV, Darvin ME. Melanin distribution from the dermal-epidermal junction to the stratum corneum: non-invasive in vivo assessment by fluorescence and Raman microspectroscopy. *Sci Rep*. 2020;10:14374.
48. Liu X, Liu T, Wen R, et al. Optical coherence photoacoustic microscopy for in vivo multimodal retinal imaging. *Opt Lett*. 2015;40:1370–1373.
49. Palczewska G, Boguslawski J, Stremplewski P, et al. Noninvasive two-photon optical biopsy of retinal fluorophores. *Proc Natl Acad Sci USA*. 2020;117:22532–22543.
50. Boguslawski J, Palczewska G, Tomczewski S, et al. In vivo imaging of the human eye using a 2-photon-excited fluorescence scanning laser ophthalmoscope. *J Clin Invest*. 2022;132. (Online print only).
51. Alagoz C, Pekel G, Alagoz N, et al. Choroidal thickness, photoreceptor thickness, and retinal vascular caliber alterations in dark adaptation. *Curr Eye Res*. 2016;41:1608–1613.
52. Su EH, Kesavamoorthy N, Ameri H. Optical coherence tomography in healthy human subjects in the setting of prolonged dark adaptation. *Sci Rep*. 2023;13:3725.
53. Gao S, Li Y, Bissig D, et al. Functional regulation of an outer retina hyporeflective band on optical coherence tomography images. *Sci Rep*. 2021;11:10260.
54. Li Y, Zhang Y, Chen S, Vernon G, Wong WT, Qian H. Light-dependent OCT structure changes in photoreceptor degenerative RD 10 mouse retina. *Invest Ophthalmol Vis Sci*. 2018;59:1084–1094.
55. Borrelli E, Costanzo E, Parravano M, et al. Impact of bleaching on photoreceptors in different intermediate AMD phenotypes. *Transl Vis Sci Technol*. 2019;8:5.
56. Jonnal RS, Besecker JR, Derby JC, et al. Imaging outer segment renewal in living human cone photoreceptors. *Opt Express*. 2010;18:5257–5270.
57. Kocaoglu OP, Liu Z, Zhang F, Kurokawa K, Jonnal RS, Miller DT. Photoreceptor disc shedding in the living human eye. *Biomed Opt Express*. 2016;7:4554–4568.


Investigative Ophthalmology & Visual Science

58. Zhang P, Shibata B, Peinado G, Zawadzki RJ, FitzGerald P, Pugh EN, Jr. Measurement of diurnal variation in rod outer segment length in vivo in mice with the OCT optoretinogram. *Invest Ophthalmol Vis Sci*. 2020; 61:9.
59. Ko GY. Circadian regulation in the retina: from molecules to network. *Eur J Neurosci*. 2020;51:194–216.
60. Pijewska E, Zhang P, Meina M, Meleppat RK, Szkulmowski M, Zawadzki RJ. Extraction of phase-based optoretinograms (ORG) from serial B-scans acquired over tens of seconds by mouse retinal raster scanning OCT system. *Biomed Opt Express*. 2021;12:7849–7871.
61. Curcio CA, Medeiros NE, Millican CL. Photoreceptor loss in age-related macular degeneration. *Invest Ophthalmol Vis Sci*. 1996;37:1236–1249.
62. Riedl S, Cooney L, Grechenig C, et al. Topographic analysis of photoreceptor loss correlated with disease morphology in neovascular age-related macular degeneration. *Retina*. 2020;40:2148–2157.
63. Si Z, Zheng Y, Zhao J. The role of retinal pigment epithelial cells in age-related macular degeneration: phagocytosis and autophagy. *Biomolecules*. 2023;13. (Online print only).
64. Boulton M, Dayhaw-Barker P. The role of the retinal pigment epithelium: topographical variation and ageing changes. *Eye (Lond)*. 2001;15:384–389.

Investigative Ophthalmology & Visual Science